Dimensionality Driven Spin-Flop Transition in Layered Iridates

J. W. Kim,[1] Y. Choi,[1] Jungho Kim,[1] J. F. Mitchell,[2] G. Jackeli,[3] M. Daghofer,[4] J. van den Brink,[4] G. Khaliullin,[3] and B. J. Kim[2,*]

[1]*Advanced Photon Source, Argonne National Laboratory, Argonne, Illinois 60439, USA*
[2]*Materials Science Division, Argonne National Laboratory, Argonne, Illinois 60439, USA*
[3]*Max Planck Institute for Solid State Research, Heisenbergstrasse 1, D-70569 Stuttgart, Germany*
[4]*Institute for Theoretical Solid Sate Physics, IFW Dresden, Helmholtzstrasse 20, 01069 Dresden, Germany*

(Received 14 May 2012; published 17 July 2012)

Using resonant x-ray diffraction, we observe an easy c-axis collinear antiferromagnetic structure for the bilayer $Sr_3Ir_2O_7$, a significant contrast to the single layer Sr_2IrO_4 with in-plane canted moments. Based on a microscopic model Hamiltonian, we show that the observed spin-flop transition as a function of number of IrO_2 layers is due to strong competition among intra- and interlayer bond-directional pseudodipolar interactions of the spin-orbit entangled $J_{\text{eff}} = 1/2$ moments. With this we unravel the origin of anisotropic exchange interactions in a Mott insulator in the strong spin-orbit coupling regime, which holds the key to the various types of unconventional magnetism proposed in $5d$ transition metal oxides.

DOI: 10.1103/PhysRevLett.109.037204 PACS numbers: 75.30.Gw, 71.70.Ej, 75.10.Dg, 75.25.−j

Despite the long history of research on magnetism in insulating oxides, magnetism in $5d$ transition-metal oxides (TMO) with strong spin-orbit coupling (SOC) is only now beginning to be explored. Since the recent discovery of the SOC-driven Mott insulator with $J_{\text{eff}} = 1/2$ states in Sr_2IrO_4 [1,2], a wide array of theoretical proposals have been put forward for novel types of quantum magnetism and topological phases of matter [3–9]. The magnetism in the strong SOC limit has two fundamentally novel aspects: (i) orbitals of different symmetries are admixed by SOC and thus the magnetic exchange interactions are multidirectional, which is evident in particular from the ''cubic'' shape of the $J_{\text{eff}} = 1/2$ Kramers doublet wave function relevant for tetravalent iridates [1–3]; (ii) the quantum phase inherent in the $J_{\text{eff}} = 1/2$ states can strongly suppress the isotropic Heisenberg coupling via a destructive interference among multiple superexchange paths and lead to large anisotropic exchange couplings of the form of pseudodipolar (PD) and Dzyaloshinsky-Moriya (DM) interactions [3]. This provides a mechanism for frustrated magnetic interactions that are predicted to lead to unconventional magnetism, such as the Kitaev model with spin liquid ground state [3,5,10]. By contrast, magnetic interactions in the weak SOC limit are predominantly of isotropic Heisenberg type weakly perturbed by the anisotropic couplings.

The central theoretical premise underlying various iridates is that the Kramers pair of $J_{\text{eff}} = 1/2$ states is the correct starting point. Strictly speaking, however, the exact $J_{\text{eff}} = 1/2$ states are realized only in cubic symmetry and in the large Coulomb correlation limit. Although it has been shown that in Sr_2IrO_4, having tetragonal symmetry at the Ir site, the ground state wave function is indeed close to the $J_{\text{eff}} = 1/2$ state [2], it is not *a priori* obvious that this should also be the case for other iridates with symmetries lower than cubic. Further, the $J_{\text{eff}} = 1/2$ states are also perturbed by the hopping term, the effect of which should be more pronounced in iridates with small charge gap such as the $Sr_3Ir_2O_7$ [11], a bilayer variant of the single layer Sr_2IrO_4. Experimentally, a clear signature of the unique features of the interactions inherent to the $J_{\text{eff}} = 1/2$ moments, e.g., strong PD couplings, has yet to be seen, especially in $(Na, Li)_2IrO_3$ [12–14], the candidate material for realization of the Kitaev model.

In this Letter, we report a direct manifestation of the strong PD interactions in $Sr_3Ir_2O_7$, which result from the $J_{\text{eff}} = 1/2$ states that are robust despite the proximity of $Sr_3Ir_2O_7$ to the metal-insulator transition (MIT) boundary. Using resonant x-ray diffraction (RXD), we find in $Sr_3Ir_2O_7$ a G-type antiferromagnetic (AF) structure [15] with c-axis collinear moments, in contrast to the ab-plane canted AF structure found for Sr_2IrO_4. The observed spin-flop transition as a function of number of IrO_2 layers does not accompany an orbital reconstruction, which shows that the strong interlayer PD couplings, supported by the three-dimensional (3D) shape of the $J_{\text{eff}} = 1/2$ wave function, are indeed responsible for the spin-flop transition. Employing the microscopic model Hamiltonian of Ref. [3], we show that in wide—and realistic—parameter ranges, the same microscopic parameters describing the $J_{\text{eff}} = 1/2$ electronic states lead to easy-ab-plane moments for the single layer Sr_2IrO_4 and c-axis collinear moments for $Sr_3Ir_2O_7$. This implies that the transition occurs only as a function of dimensionality, which is a consequence of the robustness of $J_{\text{eff}} = 1/2$ states (albeit perturbed to some extent) against strong quasi-3D hopping amplitudes.

Experiments were carried out at the 4-IDD and 6-ID beam lines at the Advanced Photon Source, with incident photon energy tuned to the Ir $L_{2,3}$ edges. A horizontal scattering geometry was used with a π-polarized incident

beam. The polarization of the scattered x rays was analyzed with pyrolytic graphite (0 0 8) and (0 0 10) reflections for the L_3 and L_2 edges, respectively. A single crystal was mounted on a closed-cycle cryostat, and data were collected at a temperature of about 5 K. No indications of change in the magnetic structure were found in the measurements repeated at 120 and 250 K. X-ray absorption spectra were recorded simultaneously in partial fluorescence mode using an energy-dispersive detector.

Figure 1 shows the magnetic structure solved in the present study along with the underlying crystal structure. $Sr_3Ir_2O_7$ was first reported to adopt the space group $I4/mmm$ [16] but was later assigned to $Bbcb$ based on single crystal diffraction and transmission electron microscopy [17–19]. In this orthorhombic structure, all neighboring octahedra are rotated in an opposite sense about the c axis, breaking inversion symmetries with respect to the shared oxygen ions and thereby allowing DM interactions.

The c-axis collinear AF structure [Fig. 1(b)] is unambiguously solved from analysis of data presented in Figs. 2 and 3. Figure 2(a) shows magnetic Bragg peaks scanned over a wide range of l, with (h, k) fixed at (1,0) and (0,1). The crystallographically forbidden $h + k =$ odd reflections imply AF ordering within an IrO_2 plane, and the observed large intensity modulation along the l direction reflects the bilayer magnetic structure factor. The magnetic peaks were refined at each l, and the corresponding intensities obtained from integrating rocking curves are plotted in Fig. 2(b). The intensity modulation has a periodicity set by the ratio between the lattice parameter c and the bilayer distance d (see Fig. 1), i.e., $c/d \approx 5.13$ and agrees well with the profile expected for AF ordering between two neighboring IrO_2 planes. Thus, it follows that all nearest-neighbor pairs are AF ordered. The fact that the l scans do not contain either (1 0 odd) or (0 1 even) reflections shows that a single magnetic domain is sampled in our measurement [15,20]. Figure 2(c) shows the temperature dependence of the intensity of (0 1 19) reflection, which disappears above ≈ 285 K and correlates with the reported anomalies in the magnetization and the resistivity data [17], implying that these anomalies are associated with the onset of long range AF ordering.

To determine the orientation of the magnetic moment, we performed polarization analysis on two magnetic Bragg peaks, as shown in Fig. 3. The (1 0 18) reflection was recorded at the azimuthal angle $\Psi = 0°$ defined such that it is zero when the reference vector (1 0 0) is in the scattering plane. The data show that (1 0 18) reflection appears only in the π-σ channel, demonstrating that the component of the magnetic moment contributing to this reflection is confined to the scattering plane defined by (1 0 0) and (1 0 18) vectors. This implies the easy axis is in the ac plane. Rotating Ψ by 90°, now (0 1 0) and (0 1 19) vectors are contained in the scattering plane. In this

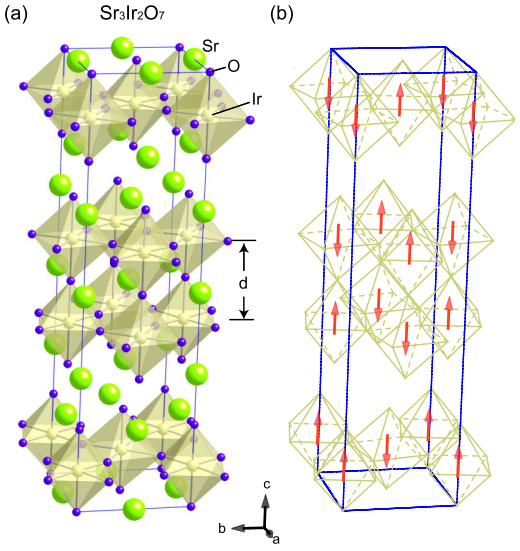

FIG. 1 (color online). (a) Crystal structure of $Sr_3Ir_2O_7$ as reported in Ref. [17]. Every neighboring IrO_6 octahedra are rotated in opposite sense about the c axis by $\simeq 12°$. (b) Magnetic order has a c-axis collinear G-type antiferromagnetic structure. The up and down magnetic moments correlate with counterclockwise and clockwise rotations of the IrO_6 octahedra, respectively.

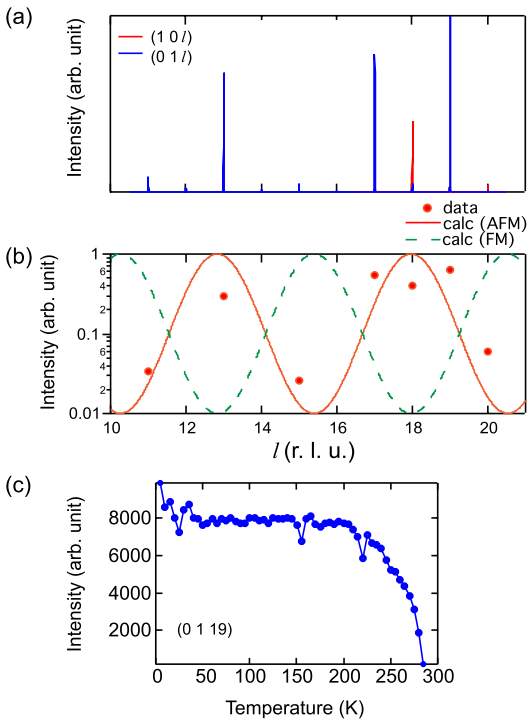

FIG. 2 (color online). (a) l scan measured in π-σ polarization channel showing magnetic Bragg peaks. (b) Integrated intensities at each peak obtained from rocking curves (red dots). Red solid (green dashed) line is bilayer structural factor expected for antiferromagnetic (ferromagnetic) alignment of two adjacent IrO_2 planes in a bilayer expressed by $\cos^2\frac{2\pi d}{c}$ ($\sin^2\frac{2\pi d}{c}$). (c) Temperature dependence of (0 1 19) peak.

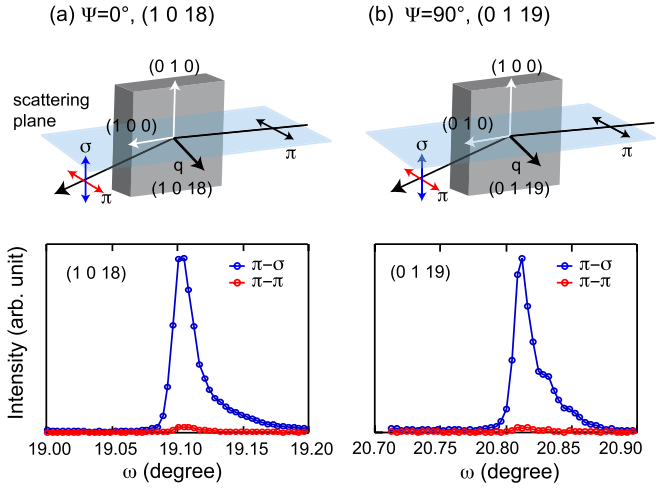

FIG. 3 (color online). Rocking curves measured in two polarization channels for (a) (1 0 18) reflection and (b) (0 1 19) reflections. The azimuth angle, defined with respect to the reference vector (1 0 0), was set at 0° for (1 0 18) reflection so that the scattering plane is defined by (1 0 0) and (1 0 18). Likewise, for (0 1 19) reflection azimuth angle was set at 90° so that the scattering plane is defined by (0 1 0) and (0 1 19).

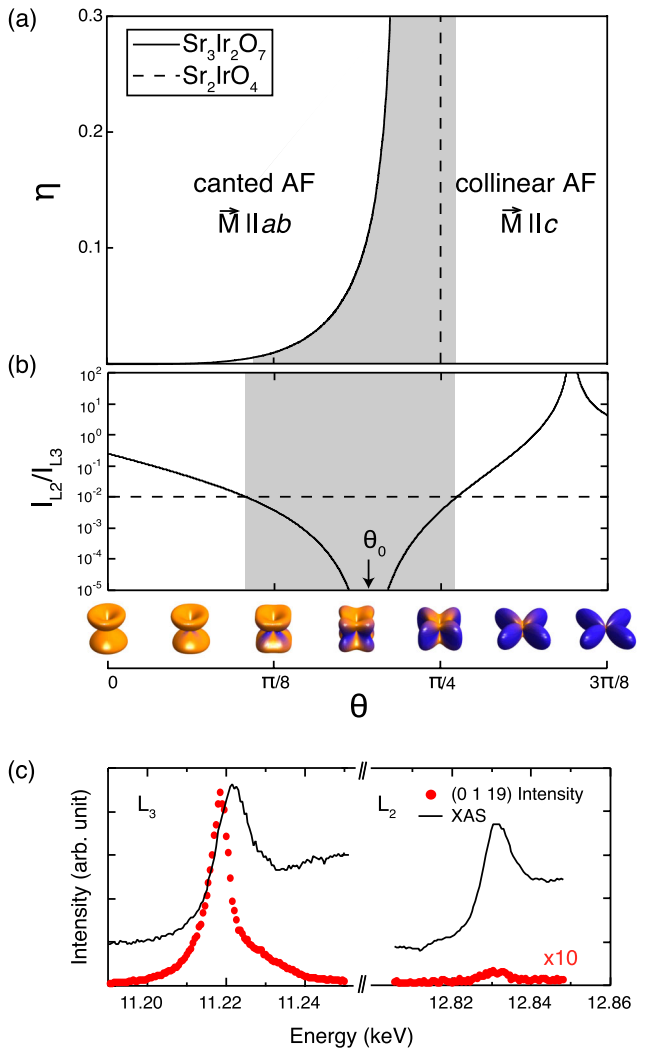

FIG. 4 (color online). (a) The ground state phase diagram of the Hamiltonian (1) in terms of $\eta = J_H/U$ and the tetragonal distortion parameter θ [the values of θ smaller (larger) than θ_0 correspond to compressed (elongated) octahedra]. The solid (dashed) line marks the spin-flop transition in bilayer (single-layer) system. The shaded area indicates the parameter space for $Sr_3Ir_2O_7$ constrained by experimental observations (see text). (b) The ratio of intensities at L_2 and L_3 calculated as a function of θ. The experimental ratio of at most 1% provides the lower and upper bounds for θ. Spin-orbital density map is shown for some values of θ with spin up (down) represented by light gray (dark gray) [orange (blue)]. (c) Energy scan of (0 1 19) reflection scanned around Ir L_3 and L_2 resonance. Red dots and black lines indicate scattering intensity and x-ray absorption spectra, respectively.

geometry, the (0 1 19) reflection also appears only in the π-σ channel, from which follows that the easy axis also lies in the bc plane. Taking these two data together, it is unambiguously determined that the magnetic Bragg peaks of (1 0 l) and (0 1 l) are associated with the c-axis component of the magnetic moment. With the provision of $\vec{k} = 0$ ordering, the magnetic structure is uniquely solved as shown in Fig. 1(b) [21].

Having determined the magnetic structure, we now analyze the origin of distinct magnetic orderings in layered iridates. In the case of single layer Sr_2IrO_4, it has been shown [3] that DM couplings can be gauged away by a proper rotation of quantization axes, and the magnetic anisotropy is solely decided by the bond-directional PD interactions whose sign and hence moment direction is controlled by the tetragonal distortion parameter θ alone (while $\eta = J_H/U$, the ratio of Hund's exchange and the local Coulomb repulsion, scales the magnitude of the PD terms and magnon gaps). In the bilayer $Sr_3Ir_2O_7$ case, however, one may expect strong interlayer couplings since the spin-orbit entangled wave function in iridates is spatially of 3D shape [1–3]. This suggests that magnetic states in iridates may strongly vary with dimensionality as number of planes are increased, unlike the case of cuprates with spin-only moments that reside on planar orbitals.

The magnetic interactions for intra- and interlayer bonds of neighboring iridium ions can be expressed in the following common form (with differing coupling constants for inter- and intralayer bonds):

$$\mathcal{H}_{ij} = J_{ij}\vec{S}_i \cdot \vec{S}_j + \Gamma_{ij}S_i^z S_j^z + \vec{D}_{ij} \cdot [\vec{S}_i \times \vec{S}_j], \quad (1)$$

where the first term stands for isotropic AF exchange J_{ij}, and the second term describes symmetric anisotropy Γ_{ij} that includes PD terms driven by Hund's exchange and those due to staggered rotations of octahedra [3]. These rotations also induce DM interaction, the third term in Eq. (1), with DM vector $\vec{D}_{ij}$ parallel to the c axis on all bonds, while its direction is staggered. For intralayer

bonds, the coupling constants are identical to those for the single layer case, derived in Ref. [3] in terms of η, θ, and the octahedra rotation angle α. We have extended the same derivation to interlayer bonds [22]; the results are presented in the Supplemental Material [23]. The Hamiltonian (1) supports two types of ordered states: a canted AF structure with moments in the ab plane and a collinear AF order with moments along the c axis, with AF interlayer stacking in both cases. We obtained a classical phase boundary between these phases marking a spin-flop transition as a function of η and θ. The result is shown as a solid line in Fig. 4(a). The dashed line in the same figure shows the spin-flop transition for the single-layer compound. It is evident that the AF order with c-axis moments has a wider stability window in the bilayer compound than in the single-layer one. One may note that the same set of parameters in the wide parameter space, bounded by the solid and dashed lines in Fig. 4(a), leads to in-plane moments for single layer Sr_2IrO_4 and c-axis moments for bilayer $Sr_3Ir_2O_7$; i.e., the spin-flop transition occurs without an accompanying "orbital" reconstruction. This transition is mostly driven by the interlayer PD term Γ_c, which favors c-axis collinear structure irrespective of the value of θ. We find that for realistic values of η and θ this term can be as large as 0.2–0.3 J, which much exceeds the PD couplings in 3D TMOs, e.g., cuprates [24].

The observed dimensionality driven spin-flop transition, which is rare in TMOs, is a natural consequence of the electronic ground state close to $J_{\text{eff}} = 1/2$ states with multidirectional [see Fig. 4(b)] and strong anisotropic couplings. Indeed, it is seen that $Sr_3Ir_2O_7$ has a similar degree of deviation from the exact $J_{\text{eff}} = 1/2$ states (for which L_2 RXD intensity is zero) as in the single layer Sr_2IrO_4 [2], as evidenced by the smallness of L_2 intensity ($I_{L_2}/I_{L_3} < 1\%$) as shown in Fig. 4(c) [25]. By contrast, in TMOs with polarized orbitals, adding another layer would generally not affect the magnetic structure unless accompanied by an orbital transition; for example, in cuprates, the planar x^2-y^2 orbitals cannot mediate strong anisotropic interlayer couplings. We find robust $J_{\text{eff}} = 1/2$ states in $Sr_3Ir_2O_7$, a system lying close to the borderline of MIT with strong hopping amplitudes and a dimensionality greater than two. The validity of the $J_{\text{eff}} = 1/2$ picture has also been confirmed recently [26] in $CaIrO_3$, a postperovskite material with edge-sharing geometry relevant to the Kitaev model, pointing out that the $J_{\text{eff}} = 1/2$ states may be more generally applicable beyond the Ruddelsden-Popper series.

It remains to be clarified how the observed c-axis collinear structure can be reconciled with the reported unusual magnetic effects, such as weak ferromagnetism, diamagnetism, and magnetoresistivity observed at rather low magnetic fields below 1 T applied in the in-plane direction [17]. A possible scenario is that the moment may be canted off from the c axis with the in-plane component appearing at different propagation vector q's. An alternative possibility is that an additional order parameter is present and is responsible for the above magnetic effects. More investigations are needed to resolve these issues.

In summary, we have revealed—through the observation of spin-flop transition in layered iridates—a direct manifestation of the PD interactions that are expected for $J_{\text{eff}} = 1/2$ states and are the essential components of the unique magnetism proposed in 5d TMOs with strong SOC. For bilayer iridate $Sr_3Ir_2O_7$, these interactions lead to the collinear AF ground state with moments directed along the c axis, in contrast to the easy-plane canted AF structure of Sr_2IrO_4. The strong dependence of magnetic structure on the number of IrO_2 planes reflects the spin-orbit entangled nature of wave functions, which are spatially of 3D shape and support strong interlayer couplings, unlike the case of, e.g., cuprates with planar orbitals. The resulting competition between intra- and interlayer PD (and also DM) interactions is tuned by the octahedral rotation and tetragonal distortion, giving rise to the moment reorientation. Our experimental confirmation of robust $J_{\text{eff}} = 1/2$ states in a system close to a MIT and their strongly non-Heisenberg interactions strengthens the expectation for novel magnetism in correlated oxides with strong SOC.

The work in the Materials Science Division and the use of the Advanced Photon Source at the Argonne National Laboratory was supported by the U.S. DOE under Contract No. DE-AC02-06CH11357. G. J. acknowledges support from GNSF/ST09-447, M. D. from the DFG (Emmy-Noether program).

*Corresponding author.
bjkim@anl.gov

[1] B. J. Kim, H. Jin, S. J. Moon, J.-Y. Kim, B.-G. Park, C. S. Leem, J. Yu, T. W. Noh, C. Kim, S.-J. Oh, J.-H. Park, V. Durairaj, G. Cao, and E. Rotenberg, Phys. Rev. Lett. **101**, 076402 (2008).
[2] B. J. Kim, H. Ohsumi, T. Komesu, S. Sakai, T. Morita, H. Takagi, and T. Arima, Science **323**, 1329 (2009).
[3] G. Jackeli and G. Khaliullin, Phys. Rev. Lett. **102**, 017205 (2009).
[4] D. Pesin and L. Balents, Nature Phys. **6**, 376 (2010).
[5] J. Chaloupka, G. Jackeli, and G. Khaliullin, Phys. Rev. Lett. **105**, 027204 (2010).
[6] X. Wan, A. M. Turner, A. Vishwanath, and S. Y. Savrasov, Phys. Rev. B **83**, 205101 (2011).
[7] F. Wang and T. Senthil, Phys. Rev. Lett. **106**, 136402 (2011).
[8] T. Hyart, A. R. Wright, G. Khaliullin, and B. Rosenow, Phys. Rev. B **85**, 140510 (2012).
[9] W. Witczak-Krempa and Y. B. Kim, Phys. Rev. B **85**, 045124 (2012).
[10] Y. Singh, S. Manni, J. Reuther, T. Berlijn, R. Thomale, W. Ku, S. Trebst, and P. Gegenwart, Phys. Rev. Lett. **108**, 127203 (2012).
[11] S. J. Moon, H. Jin, K. W. Kim, W. S. Choi, Y. S. Lee, J. Yu, G. Cao, A. Sumi, H. Funakubo, C. Bernhard, and T. W. Noh, Phys. Rev. Lett. **101**, 226402 (2008).

[12] X. Liu, T. Berlijn, W.-G. Yin, W. Ku, A. Tsvelik, Y.-J. Kim, H. Gretarsson, Y. Singh, P. Gegenwart, and J. P. Hill, Phys. Rev. B **83**, 220403 (2011).

[13] S. K. Choi, R. Coldea, A. N. Kolmogorov, T. Lancaster, I. I. Mazin, S. J. Blundell, P. G. Radaelli, Y. Singh, P. Gegenwart, K. R. Choi, S.-W. Cheong, P. J. Baker, C. Stock, and J. Taylor, Phys. Rev. Lett. **108**, 127204 (2012).

[14] F. Ye, S. Chi, H. Cao, B. C. Chakoumakos, J. A. Fernandez-Baca, R. Custelcean, T. Qi, O. B. Korneta, and G. Cao, Phys. Rev. B **85**, 180403(R) (2012).

[15] S. Boseggia, R. Springell, H. C. Walker, A. T. Boothroyd, D. Prabhakaran, D. Wermeille, L. Bouchenoire, S. P. Collins, and D. F. McMorrow, Phys. Rev. B **85**, 184432 (2012).

[16] M. A. Subramanian, M. K. Crawford, and R. L. Harlow, Mater. Res. Bull. **29**, 645 (1994).

[17] G. Cao, Y. Xin, C. S. Alexander, J. E. Crow, P. Schlottmann, M. K. Crawford, R. L. Harlow, and W. Marshall, Phys. Rev. B **66**, 214412 (2002).

[18] H. Matsuhata, I. Nagai, Y. Yoshida, S. Hara, S.-I. Ikeda, and N. Shirakawa, J. Solid State Chem. **177**, 3776 (2004).

[19] Although the space group Pban has been reported for $Sr_3Ir_2O_7$ [G. R. Blake *et al.*, ESRF Experimental Report No. HS-2386, 2004 (unpublished)], the report does not provide enough experimental data from which one could reproduce the results. We were not able to observe any Bragg reflections violating the B-centering condition $h + l = 2n$ in our sample.

[20] Although our sample consisted of several domains, these domains were sufficiently large that we could confine the probed region to a single domain. Special care has been taken to align the sample very precisely so that the beam does not move to a different domain when the sample is rotated.

[21] Magnetic structures consistent with a $k = (0, 0, 0)$ ordering in the crystallographic space group *Bbcb* (alternate setting of *Ccca*:1, No. 68) with Ir in Wyckoff position 8*e* were examined using representation theory. No magnetic structure derived from ordering according to a single irreducible representation can support both a-b and c-axis components.

[22] G. Jackeli and G. Khaliullin (unpublished).

[23] See Supplemental Material at http://link.aps.org/supplemental/10.1103/PhysRevLett.109.037204 for theory details.

[24] D. Petitgrand, S. V. Maleyev, P. Bourges, and A. S. Ivanov, Phys. Rev. B **59**, 1079 (1999).

[25] To compare scattering intensities measured at two different incident photon energies separated by more than 1 keV requires consideration of the differences in the probing depth, efficiency of I_0 monitor, and polarization analyzer. Analyzing these effects, we find that the intensity of L_2 tends to be overestimated. Therefore the measured intensity at L_2 provides the upper bound for the L_2/L_3 intensity ratio.

[26] K. Ohgushi, J. Yamaura, H. Ohsumi, K. Sugimoto, S. Takeshita, A. Tokuda, H. Takagi, M. Takata, and T. Arima, arXiv:1108.4523.